Memory/effector (CD45RB^{lo}) CD4 T cells are controlled directly by IL-10 and cause IL-22–dependent intestinal pathology

Masahito Kamanaka,[1] Samuel Huber,[1,7] Lauren A. Zenewicz,[1] Nicola Gagliani,[1] Chozhavendan Rathinam,[1] William O'Connor Jr.,[1] Yisong Y. Wan,[4,5] Susumu Nakae,[6] Yoichiro Iwakura,[6] Liming Hao,[2] and Richard A. Flavell[1,3]

[1]Department of Immunobiology, [2]Department of Pathology, and [3]Howard Hughes Medical Institute, School of Medicine, Yale University, New Haven, CT 06520
[4]Lineberger Comprehensive Cancer Center and [5]Department of Microbiology and Immunology, School of Medicine, The University of North Carolina at Chapel Hill, Chapel Hill, NC 27599
[6]Center for Experimental Medicine and Systems Biology, The Institute of Medical Science, The University of Tokyo, Minato-ku, Tokyo 108-8639, Japan
[7]I. Medizinische Klinik, Universitätsklinik Hamburg-Eppendorf, 20246 Hamburg, Germany

The role of direct IL-10 signaling in different T cell subsets is not well understood. To address this, we generated transgenic mice expressing a dominant-negative IL-10 receptor specifically in T cells (CD4dnIL-10Rα). We found that Foxp3-depleted CD45RB^{lo} (regulatory T cell [T_{reg} cell]–depleted CD45RB^{lo}) but not CD45RB^{hi} CD4$^+$ T cells are controlled directly by IL-10 upon transfer into Rag1 knockout (KO) mice. Furthermore, the colitis induced by transfer of T_{reg} cell–depleted CD45RB^{lo} CD4$^+$ T cells into Rag1 KO mice was characterized by reduced Th1 and increased Th17 cytokine messenger RNA levels in the colon as compared with the colitis induced by transfer of CD45RB^{hi} T cells. In contrast to the CD45RB^{hi} transfer colitis model, in which IL-22 is protective, we found that T cell–derived IL-22 was pathogenic upon transfer of T_{reg} cell–depleted CD45RB^{lo} T cells into Rag1 KO mice. Our results highlight characteristic differences between colitis induced by naive (CD45RB^{hi}) and memory/effector (T_{reg} cell–depleted CD45RB^{lo}) cells and different ways that IL-22 impacts inflammatory bowel disease.

CORRESPONDENCE
Richard A. Flavell:
richard.flavell@yale.edu

Abbreviations used: HPRT, hypoxanthine phosphoribosyltransferase; IBD, inflammatory bowel disease; mRNA, messenger RNA; TG, transgenic; TUNEL, TdT-mediated dUTP-biotin nick end labeling.

IL-10 is one of the most important anti-inflammatory cytokines and plays an especially critical role in the intestine. The role of IL-10 in the gut is underscored by the high expression of IL-10 by intestinal lymphocytes (Kamanaka et al., 2006). Furthermore, IL-10 KO mice develop spontaneous colitis (Kühn et al., 1993), which demonstrates that IL-10 is essential for the maintenance of the immune homeostasis in the intestine.

The key target cell of IL-10 is considered to be the APC. Thus, the profound reduction of the Th1 response that is mediated by IL-10 was concluded to be indirect, being mediated by inhibition of APCs (Fiorentino et al., 1991; Ding and Shevach, 1992) and resulting from down-regulation of NO production (Gazzinelli et al., 1992) and costimulatory cytokines and receptors such as IL-12 and CD80/CD86, respectively, in APCs (Ding et al., 1993). Direct effects of IL-10 on T cells have been less well defined, although inhibitory effects of IL-10 on T cells have been reported using human T cells (Taga et al., 1993; Schandené et al., 1994).

To address immune-regulatory mechanisms in the gut, an adoptive transfer model, which employs immune-deficient hosts, has been developed and is widely used (Powrie et al., 1994). In this model, naive CD45RB^{hi} CD4-positive

M. Kamanaka, S. Huber, and L.A. Zenewicz contributed equally to this paper.
M. Kamanaka's present address is Dept. of Medicine, Arai Hospital, Kuki, Saitama 346-0003, Japan.

The Rockefeller University Press $30.00
J. Exp. Med. Vol. 208 No. 5 1027-1040
www.jem.org/cgi/doi/10.1084/jem.20102149

T cells induce colitis upon transfer into Rag1 KO mice. The development of colitis could be prevented by coinjection of $CD4^+$ $CD45RB^{lo}$ cells; furthermore, this inhibition appeared to be IL-10 dependent, as prevention of colitis was abolished by the administration of neutralizing anti–IL-10R antibody (Asseman et al., 1999). Thereafter it was shown that the $CD4^+$ $CD45RB^{lo}$ population contains $CD25^+Foxp3^+$ regulatory T cells (T_{reg} cells), which are responsible for the regulatory activity of this subset (Asseman et al., 2003). However, T_{reg} cells do not need to secrete IL-10 for this suppression of disease (Asseman et al., 2003). In contrast, $CD45RB^{lo}$ $CD4^+$ T cells seem to be regulated in some way by IL-10 upon transfer into RAG1 KO mice, as anti–IL-10R antibody treatment induces colitis in recipients of $CD45RB^{lo}$ $CD4^+$ T cells (Asseman et al., 2003). However, based on this study, it was not clear whether IL-10 acts directly on $CD45RB^{lo}$ $Foxp3^+$ (nT_{reg} cell), $CD45RB^{lo}$ $Foxp3^-$ (T_{reg} cell–depleted $CD45RB^{lo}$) cells, or other cells present in the Rag1 KO host such as APCs, which are generally considered to be targets of IL-10 action.

In this study, we aimed to investigate direct effects of IL-10 on T cells. To that end, we generated mice in which IL-10 signaling is specifically blocked in T cells by transgenic (TG) overexpression of a dominant-negative IL-10Rα under the CD4 promoter (CD4dnIL-10Rα mice). We found that IL-10 signaling in T cells is dispensable for the maintenance of the immune homeostasis in mice kept under specific pathogen-free conditions. However, in contrast to $CD4^+$ $CD45RB^{hi}$ cells, TG T_{reg} cell–depleted $CD4^+$ $CD45RB^{lo}$ cells caused more severe disease upon transfer into Rag1 KO mice compared with respective WT cells and also escaped the control exerted by nT_{reg} cells. Further comparison of the colitis induced by $CD4^+$ $CD45RB^{hi}$ and T_{reg} cell–depleted $CD4^+$ $CD45RB^{lo}$ cell populations revealed that colitis induced by the transfer of $CD4^+$ $CD45RB^{hi}$ T cells into Rag1 KO mice exhibits a higher Th1 response compared with T_{reg} cell–depleted $CD4^+$ $CD45RB^{lo}$ cells, which showed increased Th17 response. Furthermore, the intestinal pathology that develops upon transfer of T_{reg} cell–depleted $CD4^+$ $CD45RB^{lo}$ T cells depended on T cell–derived IL-22, whereas in contrast, IL-22 was protective in the $CD45RB^{hi}$ model. The intestinal pathology induced by transfer of T_{reg} cell–depleted $CD4^+$ $CD45RB^{lo}$ cells was characterized by mucosal thickening and was associated with increased proliferation of colon epithelial cells, which was induced by IL-22.

RESULTS

Expression of IL-10Rα in T cell subsets

As the role of IL-10 signaling in T cells is not well characterized, we first determined the expression levels of IL-10Rα on the surface of naive ($CD45RB^{hi}$), memory/effector (T_{reg} cell–depleted $CD45RB^{lo}$), and nT_{reg} CD4 T cells (see Fig. 3 A). IL-10Rα expression was detectable in all of these cell subsets before any stimulation, albeit at very low levels (Fig. S1, A and B). However, the expression of the receptor was confirmed to be functional because IL-10 stimulation led to phosphorylation of Stat3 in $CD45RB^{hi}$ and T_{reg} cell–depleted $CD45RB^{lo}$ CD4 T cells at least at higher concentrations (Fig. S1 C). Stimulation of the T cells with anti-CD3 and CD28 antibodies in the presence of APCs enhanced the surface expression of IL-10Rα after 24–48 h in each population (Fig. S1, A and B). These results show that functional IL-10Rα is expressed by all CD4 T cell subsets both in the steady-state and after activation.

Generation of IL-10R dominant-negative TG mice

To analyze the role of IL-10 signaling in T cells, we generated mice in which IL-10 signaling is blocked in a cell lineage–specific manner. We used the same combination of the CD4 promoter and 3′ untranslated region/polyA sequences that we used previously in TGF-β RII dominant-negative TG mice (Gorelik and Flavell, 2000) to generate IL-10Rα dominant-negative mice (CD4dnIL-10Rα mice; Fig. 1 A). As reported previously, this promoter fragment lacks the regulatory element, which suppresses the expression of the transgene in CD8 T cells (Sawada et al., 1994). Consequently, the transgene is expressed in both $CD4^+$ and $CD8^+$ T cells. We obtained eight lines of TG mice. Of these lines, two had significantly higher transgene expression. As both the expression level and the initial analysis of the phenotype did not differ between these two lines, we chose one of these TG lines for further experiments and backcrossed this to the C57BL/6 background for >12 generations. TG mice developed normally and were fertile. They did not develop spontaneous intestinal inflammation even after they were backcrossed for >10 generations to the NOD/ShiLtj or BALB/c backgrounds.

First, we determined the cell surface expression levels of the transgene-encoded IL-10Rα on lymphocytes to confirm the specific expression of the IL-10Rα dominant-negative gene product in T cells. Of note, the antibody used for these experiments binds to both the TG and the WT IL-10Rα. The IL-10Rα levels on the surface of CD4 and CD8 T cells were found to be high in the TG mice (Fig. 1 B). As endogenous IL-10Rα messenger RNA (mRNA) was not altered in the TG T cells (unpublished data), the high IL-10Rα expression on T cells detected in this experiment was inferred to be the result of the expression of the TG dominant-negative receptor. The IL-10Rα expression level in B cells was slightly elevated in the TG mice. This is in line with the report by others that the CD4 promoter fragment also expresses weakly in B cells (Sawada et al., 1994). However, there was no significant increase in IL-10Rα expression in $CD4^+$ or $CD8^+$ $CD11c^+$ dendritic cells from the spleen (Fig. 1 C) or $CD11b^+$ spleen and peritoneal macrophages (not depicted).

To functionally validate the specificity of the blockade of IL-10 signaling in this TG model, we determined the phosphorylation status of Stat3 in T cells after incubation with exogenous IL-10 in vitro. In T cells from the TG mice, Stat3 phosphorylation was almost completely blocked, whereas in B cells, its phosphorylation was not affected (Fig. 1 D). Thus, T cells but not B cells from CD4dnIL-10Rα mice are poorly responsive to IL-10 signaling.

To confirm the blockade of IL-10 signaling in T cells, we measured the proliferation of thymocytes in response to IL-10 in

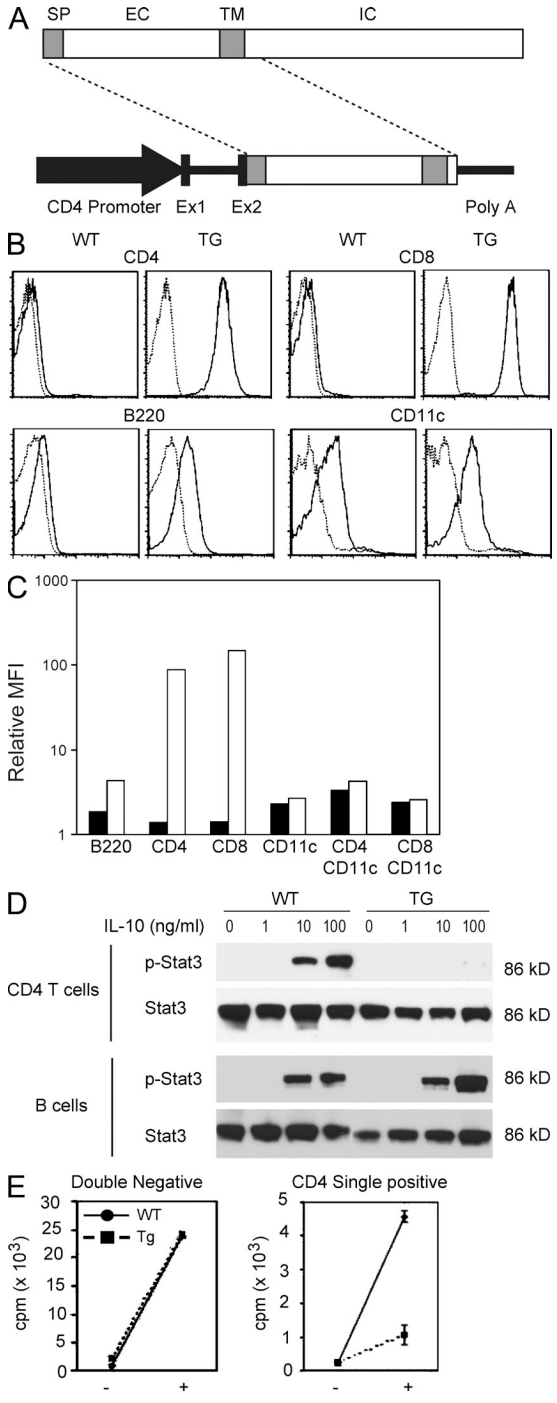

Figure 1. Generation of dominant-negative IL-10Rα TG mice. (A) Construct used for the generation of IL-10Rα dominant-negative mice. Signal peptide (SP), extracellular (EX), transmembrane (TM), and intracellular (IC) regions are shown. Ex1 and Ex2 are the exons of the CD4 promoter region. (B) Expression analysis of IL-10Rα in the dominant-negative TG mice in splenocytes. IL-10Rα expression (solid lines) was analyzed using flow cytometry. PE-conjugated hamster IgG1 was used as a control (dotted lines). (C) Relative mean fluorescence intensity (MFI) from WT mice (closed bars) and TG mice (open bars) shown as a fold increase compared with the control staining. (D) Western blot analysis of Stat3 and phospho-Stat3 (p-Stat3) in CD4 T cells and B cells incubated with the indicated concentration of IL-10. (E) CD4CD8 double-negative cells and CD4 single-positive cells were isolated from the thymus of WT and TG mice using FACS, and 10^5 cells were incubated with or without 100 ng/ml IL-10 for 5 d (indicated as + and −). [^{3}H]thymidine was added during the last 16 h of culture, and ^{3}H uptake was measured (mean ± SD of the triplicates). Results are representative of two experiments.

the TG mouse as previously described (MacNeil et al., 1990). Thymocytes from WT mice proliferated vigorously when stimulated with IL-10, whereas those from CD4dnIL-10Rα mice were much less responsive to IL-10 (Fig. 1 E). In B cells, which are known to up-regulate MHC class II in response to IL-10, as expected, we did not observe any difference in the up-regulation of these molecules (unpublished data). Thus, IL-10 signaling is specifically blocked in T cells in this TG model.

The IL-6–Stat3 pathway was not affected by the blockade of IL-10 signaling

IL-6 is an important factor that together with TGF-β induces Th17 cells (Veldhoen et al., 2006). IL-6 uses the Stat3 pathway, which is also activated by IL-10 signaling (Zhong et al., 1994). Thus, we asked whether IL-6–mediated Stat3 phosphorylation is affected by the blockade of IL-10 signaling. However, the phosphorylation of Stat3 by IL-6 was unaffected in TG CD4 T cells (Fig. S2 A). Additionally, the differentiation of Th17 cells in vitro by IL-6 and TGF-β also did not present any difference between WT and TG CD4 T cells (Fig. S2 B). Therefore, the TG overexpression of a dominant-negative IL-10Rα does not seem to alter the IL-6–Stat3 signaling pathway.

Direct IL-10 signaling in CD4$^+$ CD45RB^{lo} T cells controls colitis development

To understand the role of direct IL-10 signaling in CD4 T cells in vivo, we used the colitis model induced by adoptive transfer of CD4$^+$ T cells. First, we isolated CD4$^+$ T cells from the spleen and adoptively transferred them into syngeneic Rag1-deficient mice. Unfractionated CD4 T cells containing CD45RB^{hi}, T_{reg} cell–negative CD45RB^{lo}, and nT_{reg} cells from WT mice were not pathogenic, whereas transfer of the CD4 T cells from CD4dnIL-10Rα mice caused colitis (Fig. 2, A and B).

To further identify which CD4 T cell population was responsible for colitis development upon transfer of these TG T cells, we fractionated the CD4 T cells into CD45RB^{hi} and CD45RB^{lo} cells; the latter population consists of memory/effector CD4 T cells and nT_{reg} cells (Fig. 2 C). Rag1 KO mice adoptively transferred with CD4$^+$ CD45RB^{hi} cells from WT and TG mice both developed colitis rapidly with a similar rate of loss of body mass (Fig. 2 D). In contrast, Rag1 KO mice transferred with total CD4$^+$ CD45RB^{lo} cells from WT mice did not develop colitis, whereas the corresponding cells from the TG mice precipitated colitis in recipient mice (Fig. 2, E–G). Histological analysis confirmed the development of colitis in TG CD45RB^{lo} recipient mice (Fig. 2, F and G). These results indicate that IL-10 signaling in T cells is required to control CD45RB^{lo} but not CD45RB^{hi} cells upon transfer into Rag1 KO mice.

Foxp3$^-$CD45RB^{lo} cells, which cannot respond to IL-10, escape control by T_{reg} cells

Previously, we generated internal ribosomal entry site RFP Foxp3 knockin reporter mice (FIR mice; Wan and Flavell, 2005), which enable the identification and isolation of Foxp3-expressing cells without fixation. This reporter system is more advantageous than anti-CD25 mAb staining because CD25 is also expressed in Foxp3-negative activated cells and some Foxp3-positive cells are CD25 negative. By using these Foxp3 knockin reporter mice, CD4$^+$ CD45RB^{lo} cells could be further fractionated into Foxp3$^+$CD45RB^{lo} cells (nT_{reg} cells) and Foxp3$^-$CD45RB^{lo} (T_{reg} cell–depleted CD45RB^{lo}) cells. The gates were set for these populations as shown in Fig. 3 A. The frequency of each population did not differ significantly between WT and TG mice. As shown in Fig. 2, IL-10 signaling in total CD4 T cells was required to control them upon transfer into Rag1 KO mice. To identify whether IL-10 directly controls Foxp3$^+$CD45RB^{lo} or Foxp3$^-$CD45RB^{lo} or CD45RB^{hi} cells, we performed adoptive transfer of these three separate populations into Rag1 KO mice. Transfer of WT or TG nT_{reg} cells caused neither loss of mass nor intestinal disease (Fig. 3 B). When CD4$^+$ CD45RB^{hi} T cells from WT or TG mice were adoptively transferred, both cell populations induced similar rapid colitis (Fig. 3 B). In contrast, Rag1 KO mice that received TG CD4$^+$ CD45RB^{lo} T cells lost mass more dramatically and induced more severe colitis compared with WT (Fig. 3 B; $P < 0.05$). We next tested whether IL-10 signaling in T_{reg} cells is required for their in vivo suppressive function. Disease caused by transfer of CD4$^+$ CD45RB^{hi} T cells could be prevented by coinjection of both WT and TG T_{reg} cells (Fig. 3 C). Additionally, T_{reg} cell–mediated suppression of CD4$^+$ CD45RB^{hi} T cells was not dependent on IL-10 signaling in CD4$^+$ CD45RB^{hi} T cells (Fig. 3 D). In contrast, colitis caused by transfer of TG T_{reg} cell–depleted CD4$^+$ CD45RB^{lo}

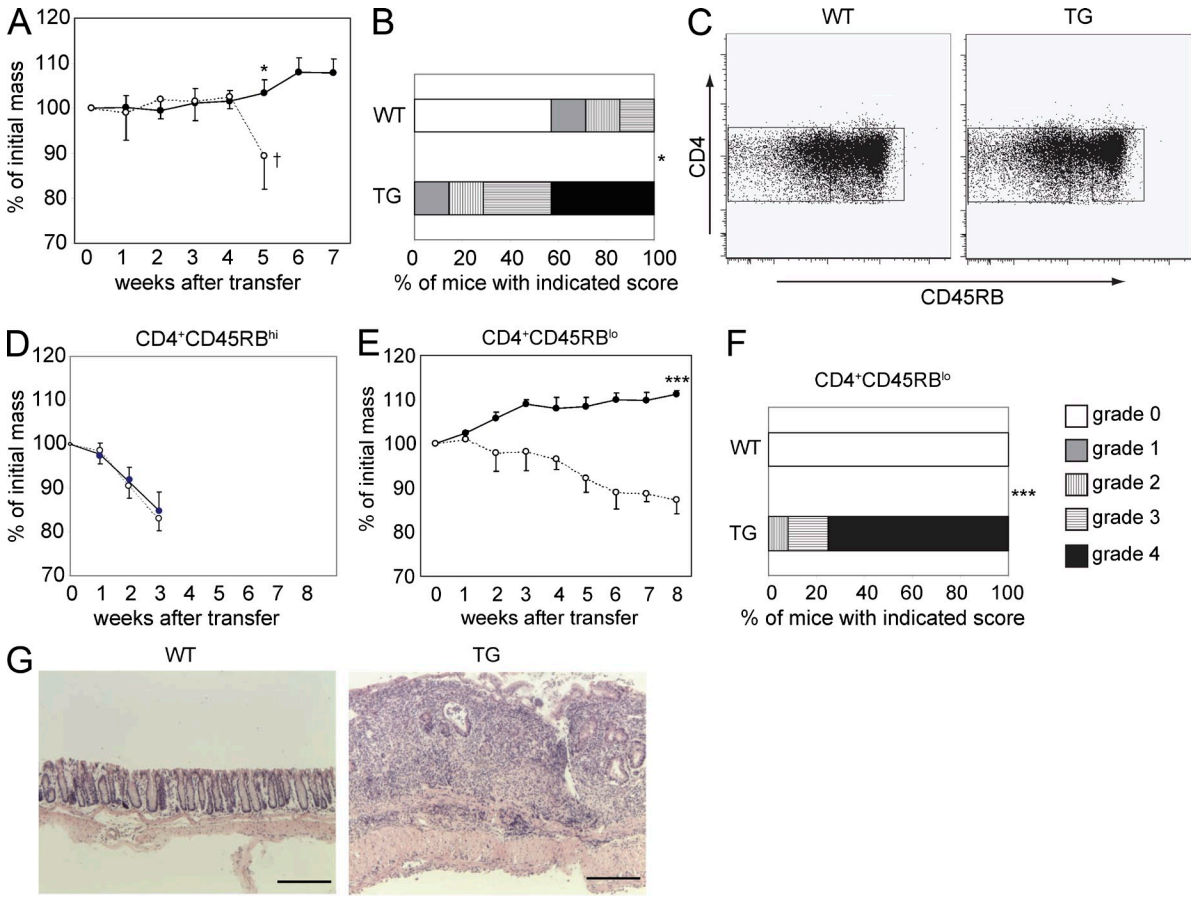

Figure 2. IL-10 controls CD45RB^{lo} cells upon transfer into Rag1 KO mice. (A) 10^6 CD4 T cells were adoptively transferred into Rag1 KO mice, and the weight changes were monitored (TG, dotted line with open circles; WT, solid line with closed circles; TG, $n = 5$; WT, $n = 5$; *, $P < 0.05$). † indicates the experiment was stopped because of the severe colitis in mice receiving CD4dnIL-10Rα T cells. (B) The histological colitis scores of colons after the adoptive transfer of total CD4$^+$ T cells (*, $P < 0.05$). (C) Representative dot plots showing the sorting gates for CD45RB^{hi} or CD45RB^{lo} cells in CD4 T cells from WT and CD4dnIL-10Rα mice. (D) 5×10^5 CD4$^+$ CD45RB^{hi} cells were adoptively transferred into Rag1 KO mice, and weight changes were monitored (TG, dotted line with open circles; WT, solid line with closed circles). (E) 5×10^5 CD4$^+$ CD45RB^{lo} cells were adoptively transferred into Rag1 KO mice, and weight changes were monitored (open circles, mice transferred with TG cells, $n = 4$; closed circles, mice transferred with WT cells, $n = 4$; ***, $P < 0.0001$). (A, D, and E) Error bars represent mean ± SEM. (F and G) Histological findings (G) and colitis score (F) of Rag1 KO transferred with CD4$^+$ CD45RB^{lo} T cells 8 wk after the transfer (WT, $n = 14$; TG, $n = 12$; ***, $P < 0.0001$). Results are representative of at least two independent experiments. Bars, 1,000 µm.

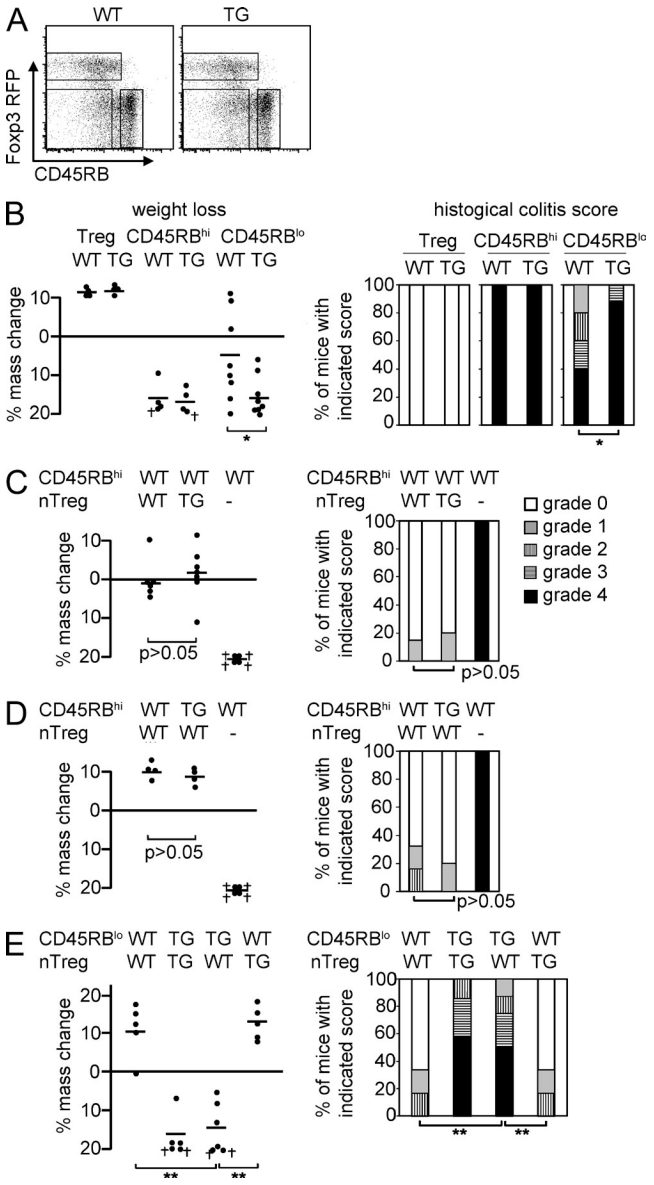

Figure 3. Foxp3$^-$CD45RB^{lo} T cells are controlled by nT$_{reg}$ cells via IL-10. (A) Representative dot plots showing the sorting gates for WT and CD4dnIL-10Rα CD4 T cell subsets. (B) 3 × 10^5 nT$_{reg}$ cells, CD45RB^{hi}, and Foxp3$^-$CD45RB^{lo} (T$_{reg}$ cell–depleted CD45RB^{lo}) CD4$^+$ T cells isolated from WT and CD4dnIL-10Rα mice were transferred into Rag1 KO mice. Weight loss and histological colitis score 6 wk after the transfer in the case of CD45RB^{hi} cell and 12 wk after transfer in the case of nT$_{reg}$ cells and T$_{reg}$ cell–depleted CD45RB^{lo} cells are shown. (C) WT and TG nT$_{reg}$ cells were transferred either alone or together with WT CD45RB^{hi} cells into Rag1 KO mice. (D) WT or TG CD45RB^{hi} cells were transferred together with WT nT$_{reg}$ cells into the Rag1 KO mice. WT CD45RB^{hi} cells were also transferred alone as a control. (E) WT or TG T$_{reg}$ cell–depleted CD45RB^{lo} cells were transferred together with WT or TG nT$_{reg}$ cells into Rag1 KO mice. (C–E) Weight change and colitis score 12 wk after the transfer are shown. (B–E) † indicates mice that had to be sacrificed because of the severity of disease. Each dot represents one animal. Horizontal bars indicate the mean. The results shown are representative of three experiments. *, P < 0.05; **, P < 0.01.

T cells could not be prevented by nT$_{reg}$ cells (Fig. 3 E). These results indicated that direct IL-10 signaling is required to control T$_{reg}$ cell–depleted CD45RB^{lo} but not CD45RB^{hi} CD4$^+$ T cells.

In vitro suppression of CD45RB^{hi} and Foxp3$^-$CD45RB^{lo} CD4$^+$ T cells by nT$_{reg}$ cells

To further investigate the mechanism of suppression by nT$_{reg}$ cells, we used the well characterized in vitro suppression assay system. As IL-23 plays an important role for the development of intestinal pathology in mice (Ahern et al., 2010) and humans (Duerr et al., 2006), we combined this assay with the addition of IL-23. First, we used CD4$^+$ CD45RB^{hi} T cells from WT or TG mice as responder cells and added varying numbers of WT nT$_{reg}$ cells to the culture wells. The suppression of proliferation by nT$_{reg}$ cells was comparable using responder WT or TG CD4$^+$ CD45RB^{hi} T cells as responders (Fig. 4, top). This suppressive effect was unaffected by the addition of IL-23. Second, we used T$_{reg}$ cell–depleted CD4$^+$ CD45RB^{lo} T cells from WT and TG mice as responder cells. nT$_{reg}$ cells again effectively suppressed T$_{reg}$ cell–depleted CD4$^+$ CD45RB^{lo} T cells. However, the addition of IL-23 rendered the cells more resistant to suppression by nT$_{reg}$ cells. This escape from suppression through IL-23 was significantly higher for the TG T cells than for WT cells (Fig. 4, middle). Of note, there was no difference in *Il23r* mRNA expression between WT and TG T$_{reg}$ cell–depleted CD4$^+$ CD45RB^{lo} T cells (Fig. S3 A). Lastly, we compared the efficiency of suppression by WT and TG nT$_{reg}$ cells using WT CD4$^+$ CD45RB^{hi} T cells as responders. nT$_{reg}$ cells from WT and TG mice could both suppress proliferation similarly in the presence or absence of IL-23. These results were consistent with the findings from adoptive transfer experiments and suggest that the blockade of IL-10 signaling may enable the T$_{reg}$ cell–depleted CD4$^+$ CD45RB^{lo} T cells to escape nT$_{reg}$ cell suppression in the presence of IL-23. However, the addition of IL-23 did not completely abrogate the suppressive capacity of nT$_{reg}$ cells, indicating that other microenvironmental factors may also contribute to the increased pathogenicity of TG T$_{reg}$ cell–depleted CD4$^+$ CD45RB^{lo} T cells upon transfer into Rag1 KO mice.

Increased pathogenicity of TG T$_{reg}$ cell–depleted CD4$^+$ CD45RB^{lo} T cells is caused by a cell-intrinsic effect

We next aimed to determine whether TG T$_{reg}$ cell–depleted CD4$^+$ CD45RB^{lo} T cells demonstrated a more pathogenic phenotype compared with WT before the transfer into Rag1 KO mice. To that end, we characterized the cytokine status of TG and WT T$_{reg}$ cell–depleted CD4$^+$ CD45RB^{lo} T cells before the adoptive transfer into Rag1 KO mice. We could not find any significant difference in IL-17A, IFN-γ, TNF-α, or IL-10 mRNA expression between freshly isolated TG and WT T$_{reg}$ cell–depleted CD4$^+$ CD45RB^{lo} T cells (Fig. S3 A). In line with this observation, we did not find a significant difference in the frequency of IL-17A–, IFN-γ–, or TNF-α–producing T$_{reg}$ cell–depleted CD4$^+$ CD45RB^{lo} T cells using intracellular cytokine staining after 3 h of activation or 4 d of stimulation

in vitro (Fig. S3 B). Additionally, ROR-γt expression at both the protein and mRNA levels was comparable between TG and WT T_{reg} cell–depleted $CD4^+$ $CD45RB^{lo}$ T cells (Fig. S3, A and C) before the transfer.

To ensure that the increased pathogenicity of TG $CD4^+$ $CD45RB^{lo}$ T cells was not caused by a difference in the in vivo environment of TG mice, which might lead to an increase of flora-reactive potentially pathogenic cells in the T_{reg} cell–depleted $CD4^+$ $CD45RB^{lo}$ T cell pool, we used a bone marrow chimera system. For this experiment, we used CD25 as a marker for T_{reg} cells. Through this approach, we were therefore able to isolate WT and TG $CD4^+CD25^-CD45RB^{lo}$ T cells, which developed in the same in vivo environment. This system allowed us to elucidate whether the increased pathogenicity of TG T_{reg} cell–depleted $CD4^+$ $CD45RB^{lo}$ T cells was caused by a cell-intrinsic effect (by the blockade of IL-10Rα on T cells) or cell-extrinsic effect (by the in vivo environment during T cell development). We generated bone marrow chimeras using mixed bone marrow from TG and WT mice injected into irradiated CD45.1 Rag1 KO mice (Fig. 5 A). 12 wk later, the cells were recovered from these mice and analyzed. The frequency of $CD45.1^+$ and $CD45.2^+$ $CD4^+$ T cells, as well as the frequency and number of $CD4^+CD25^-CD45RB^{lo}$ within $CD45.1^+$ WT and $CD45.2^+$ TG CD4 T cells, recovered from the chimeric mice was not different (Fig. 5 B and not depicted). We next isolated $CD45.1^+$ and $CD45.2^+$ $CD4^+CD25^-CD45RB^{lo}$ cells and transferred these cells into another Rag1 KO recipient. Rag1 KO mice, which received TG $CD45.2^+CD4^+CD25^-CD45RB^{lo}$ T cells, lost more body weight than the corresponding mice that received WT $CD45.1^+CD4^+CD25^-CD45RB^{lo}$ cells (Fig. 5 C). The severity of colitis assessed by endoscopic analysis also indicated that the TG T_{reg} cell–depleted $CD4^+$ $CD45RB^{lo}$ T cells induced more severe colitis compared with WT cells (Fig. 5, D and E). Our results therefore demonstrate that blockade of IL-10 signaling in T_{reg} cell–depleted $CD4^+$ $CD45RB^{lo}$ T cells induces more severe colitis in the adoptive transfer model into the Rag1 KO mice. This seems to be mediated via a T cell–intrinsic effect.

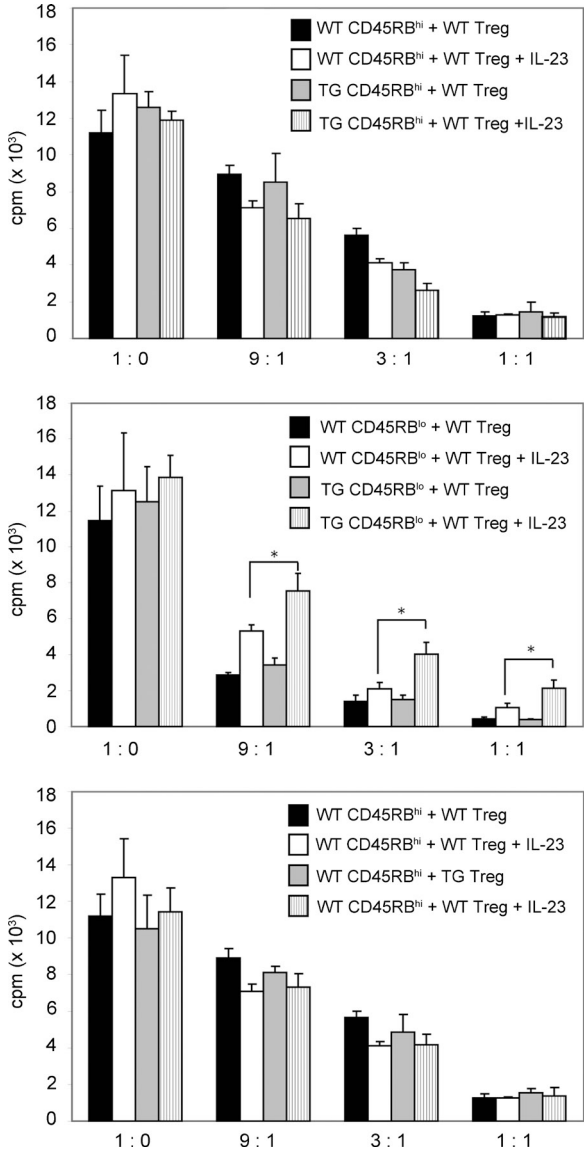

Figure 4. IL-10 signaling in Foxp3-depleted $CD45RB^{lo}$ T cells is important for their complete suppression by nT_{reg} cells in the presence of IL-23 in vitro. WT or TG $CD45RB^{hi}$ cells (top), WT or TG $CD4^+Foxp3^-CD45RB^{lo}$ (T_{reg} cell–depleted $CD45RB^{lo}$) cells (middle), or WT $CD45RB^{hi}$ cells (bottom) were cultured with WT or TG nT_{reg} cells in the presence or absence of IL-23. [^{3}H]thymidine was added during the last 16 h of culture, and ^{3}H uptake was measured. Results are representative of three experiments. Error bars represent mean ± SEM. *, $P < 0.05$.

To further prove a cell-intrinsic effect, we performed competitive adoptive transfer of $CD45RB^{hi}$ and T_{reg} cell–depleted $Foxp3^-CD45RB^{lo}$ $CD4^+$ T cells from WT and TG mice. CD45.1 was again used as a marker to distinguish the donor WT ($CD45.2^+$) or TG ($CD45.1^+/CD45.2^+$) T cells that were coinjected into Rag1 KO mice ($CD45.1^+$; Fig. S4 A). After 1 mo, proliferation of the donor T cells was measured by BrdU uptake. The $CD45RB^{hi}$ $CD4^+$ T cells from WT and TG mice proliferated similarly (Fig. S4 B, top left). However, T_{reg} cell–depleted $CD4^+$ $CD45RB^{lo}$ T cells from TG mice proliferated more than those from WT mice (Fig. S4 B, left). Supporting this observation, the ratio of WT versus TG donor $CD4^+$ T cells was almost equal if $CD45RB^{hi}$ cells were transferred, but more than twice the number of TG cells was recovered when T_{reg} cell–depleted $CD45RB^{lo}$ T cells were transferred (Fig. S4 C). This indicates that IL-10 signaling in T_{reg} cell–depleted $CD45RB^{lo}$ cells but not $CD45RB^{hi}$ $CD4^+$ T cells is required to control their proliferation. Additionally, these data again indicate a cell-intrinsic rather than a cell-extrinsic effect.

Cytokine profiles in colitis induced by $CD45RB^{hi}$ and T_{reg} cell–depleted $CD45RB^{lo}$ $CD4^+$ T cells

To further understand the characteristics of the $CD45RB^{hi}$ and T_{reg} cell–depleted $CD45RB^{lo}$ $CD4^+$ T cell transfer models and the effect of the blockade of IL-10 signaling, we measured the levels of cytokine mRNAs in the colons of diseased mice,

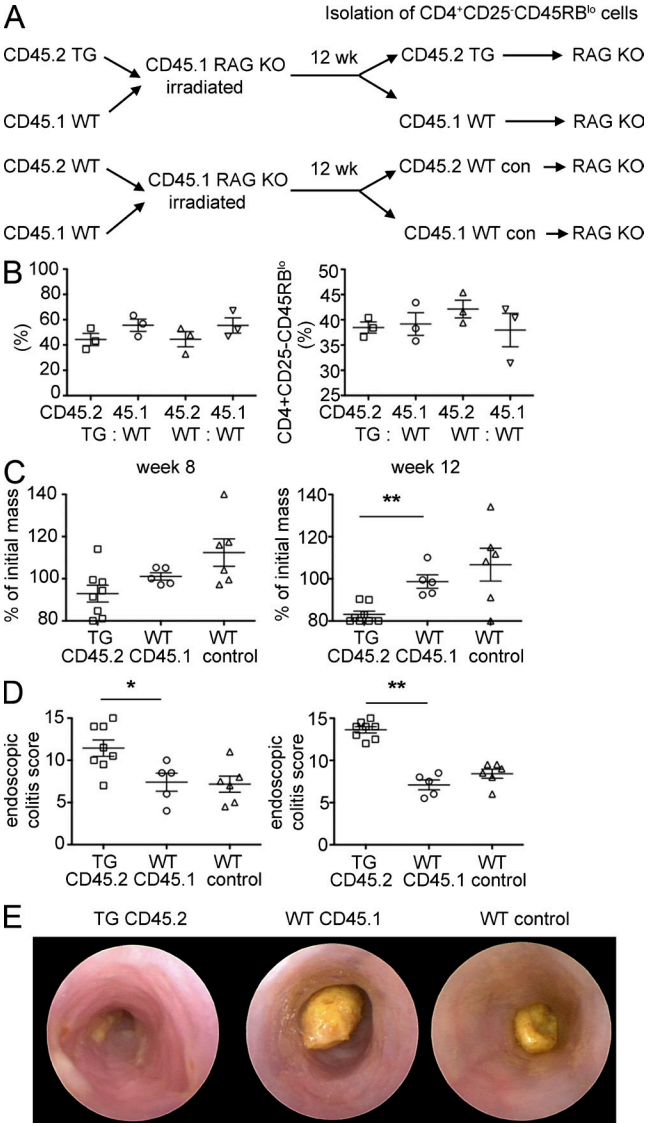

Figure 5. Increased pathogenicity of TG CD25$^-$CD45RB^{lo} cells is caused by a cell-intrinsic effect. (A) Mixed bone marrow chimeras were generated by the cotransfer of bone marrow derived from CD45.1 WT and CD45.2 WT or CD45.2 TG mice into sublethally irradiated CD45.1 Rag1 KO mice. 12 wk after the transfer, CD4$^+$CD25$^-$CD45RB^{lo} (T_{reg} cell–depleted CD45RB^{lo}) expressing either CD45.1 or CD45.2 were isolated from the spleen of chimeric mice and transferred into another Rag1 KO recipient (2×10^5). (B) Frequency of CD45.2- and CD45.1-positive cells within CD4 T cells and of CD4$^+$CD25$^-$CD45RB^{lo} cells gated on CD4$^+$CD45.1 or CD4$^+$CD45.2 cells in the spleen of chimeric mice 12 wk after transfer. (C and D) Mass loss (C) and endoscopic colitis score (D) of Rag1 KO recipients 8 and 12 wk after the transfer of CD4$^+$CD25$^-$CD45RB^{lo} cells isolated from the mixed bone marrow chimera (WT control, Rag1 KO mice receiving CD45.2 or CD45.1 WT cells isolated from the WT control chimera). (E) Representative endoscopic findings 12 wk after the transfer. Results were combined from two independent experiments. Each dot represents one animal. Error bars represent mean ± SEM. *, $P < 0.05$; **, $P < 0.01$.

which received either of these cell populations derived from WT animals. Of note, even WT T_{reg} cell–depleted CD45RB^{lo} CD4$^+$ T cells caused colitis upon transfer into Rag1 KO mice after 10–13 wk (see Fig. 8).

IFN-γ was similarly highly expressed in the CD45RB^{hi} T cell transfer model developed both by WT and TG cells (Fig. 6 A). However, the expression of IFN-γ in the WT T_{reg} cell–depleted CD4$^+$ CD45RB^{lo} T cell transfer model was less than in the CD45RB^{hi} cell transfer model. T_{reg} cell–depleted CD4$^+$ CD45RB^{lo} T cells from TG mice caused higher expression of IFN-γ in the colon of the recipient than mice that received the corresponding WT cells. IL-17A expression was higher in the mice that received T_{reg} cell–depleted CD4$^+$ CD45RB^{lo} T cells than those that received CD45RB^{hi} CD4$^+$ T cells. Furthermore, the mice that received TG T_{reg} cell–depleted CD4$^+$ CD45RB^{lo} T cells showed higher expression of IL-17A than mice that received corresponding WT cells. These results indicate that, in general, CD45RB^{hi} CD4$^+$ T cell–induced colitis is characterized by a greater Th1 response, whereas T_{reg} cell–depleted CD4$^+$ CD45RB^{lo} T cells induce a more Th17-driven colitis. Th17 cells are also known to produce IL-17F and IL-22. Because the T_{reg} cell–depleted CD45RB^{lo} colitis showed a more pronounced Th17 response, we measured these cytokines in the colons; Rag1 KO mice that received T_{reg} cell–depleted CD4$^+$ CD45RB^{lo} T cells showed increased mRNA levels of these cytokines in the colon after development of disease compared with CD45RB^{hi} cells. Also, the blockade of IL-10 signaling enhanced this effect (Fig. 6 A). These results suggest again that T_{reg} cell–depleted CD45RB^{lo} T cells generated a more Th17 cell–mediated colitis compared with CD45RB^{hi} CD4$^+$ T cells. The blockade of IL-10 signaling in T_{reg} cell–depleted CD45RB^{lo} led to more severe disease in the Rag1 KO recipient (Fig. 3), and in line with that, we also found higher IL-17F and IL-22 mRNA levels in their colons. G-CSF was reported to be induced in epithelial cells by IL-17A (Ye et al., 2001). According to our results, G-CSF mRNA expression showed a similar pattern to the other Th17 cytokine mRNA levels, which underlined the distinct cytokine patterns of the colitis induced with CD45RB^{hi} and T_{reg} cell–depleted CD45RB^{lo} CD4$^+$ T cells.

To further confirm that transfer of T_{reg} cell–depleted CD4$^+$ CD45RB^{lo} T cells into Rag1 KO mice led to a more Th17 cell–mediated colitis, we recovered CD4 T cells from the colons of Rag1 KO mice adoptively transferred with CD45RB^{hi} and T_{reg} cell–depleted CD45RB^{lo} CD4$^+$ T cells. Consistent with the higher Th17 cytokine mRNA levels, we found a higher percentage of ROR-γt–expressing cells in the mice that received T_{reg} cell–depleted CD45RB^{lo} cells compared with those receiving CD45RB^{hi} CD4$^+$ T cells (Fig. 6 B, top vs. bottom). Again, the mice that received TG T_{reg} cell–depleted CD4$^+$ CD45RB^{lo} T cells showed a further increase in the percentage of ROR-γt–expressing T cells compared with WT (Fig. 6 B, bottom). The absolute number of ROR-γt–expressing cells recovered from the colons confirmed the more pronounced development of ROR-γt–expressing T cells from the TG T_{reg} cell–depleted CD4$^+$ CD45RB^{lo} T cells than

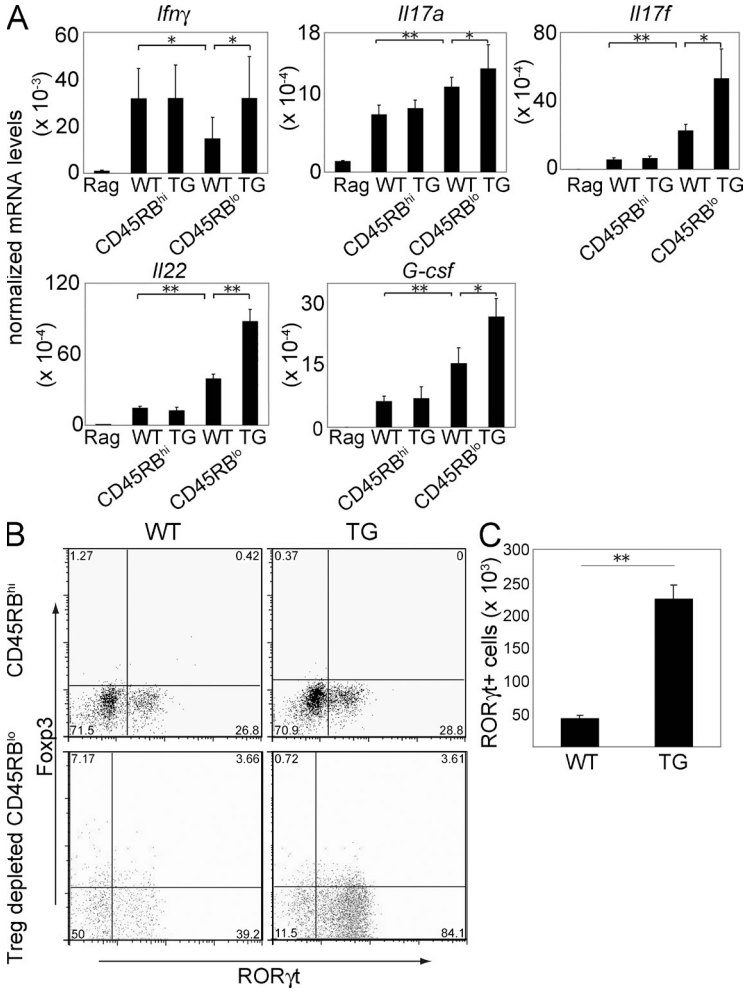

Figure 6. Increased Th17 cell cytokine profile in the inflamed colon of Rag1 KO mice adoptively transferred with Foxp3$^-$CD45RB^{lo} cells compared with recipients of CD45RB^{hi} cells. (A) mRNA levels of the indicated cytokines were measured in total colon extracts of untreated or Rag1 KO mice adoptively transferred with WT or TG CD45RB^{hi} or CD4$^+$Foxp3$^-$CD45RB^{lo} (T_{reg} cell–depleted CD45RB^{lo}) cells. mRNA levels were normalized to HPRT. Results shown represent the mean of four to eight mice per group. The experiments were repeated twice with similar results. Mononuclear cells were isolated from the colon of Rag1 KO mice (CD45.1$^+$) adoptively transferred with WT or TG CD45RB^{hi} or T_{reg} cell–depleted CD45RB^{lo} cells (CD45.2$^+$) 4–8 wk after the transfer. (B) Representative dot blots for ROR-γt and Foxp3 expression (top, Rag1 KO mice received CD45RB^{hi} WT or TG cells; bottom, Rag1 KO mice received WT or TG T_{reg} cell–depleted CD45RB^{lo} cells). Cells were gated on CD45.2$^+$ cells. (C) Number of CD4$^+$ROR-γt$^+$ cells recovered from the colon of Rag1 KO recipients of WT or TG T_{reg} cell–depleted CD45RB^{lo} cells. The experiments were repeated twice with similar results. Error bars represent mean ± SEM. *, $P < 0.05$; **, $P < 0.01$.

WT (Fig. 6 C). Of note, the percentage of ROR-γt–expressing cells before the transfer into Rag1 KO mice was very low and about the same in WT and TG T_{reg} cell–depleted CD4$^+$ CD45RB^{lo} T cells (Fig. S3 C), indicating that the large difference in ROR-γt–expressing T cell numbers obtained from colons of the adoptively transferred Rag1 KO was caused by an expansion of this cell population after transfer. In conclusion, the T_{reg} cell–depleted CD4$^+$ CD45RB^{lo} T cell–induced colitis was characterized by a greater Th17 cell response. Blockade of IL-10 signaling in T cells led to increased colitis severity in the T_{reg} cell–depleted CD4$^+$ CD45RB^{lo} colitis model, which was also associated with increased numbers of Ror-γt–positive T cells in the colon.

We next asked whether IL-10 affects the differentiation of naive T cells into Th17 cells or, alternatively, whether it acts on the antigen-experienced T cells, thereby controlling the accumulation of ROR-γt–positive T cells. IL-10 did not inhibit the differentiation of naive T cells into Th17 cells (Fig. 7 A). In contrast, we found that IL-10 decreased *Rorc* but not *Tbx21* mRNA expression in IL-23–stimulated T_{reg} cell–depleted CD4$^+$ CD45RB^{lo} in vitro (Fig. 7 B).

However, it should be noted that we found both elevated IFN-γ and IL-17A mRNA levels in the colon of Rag1 KO mice, which had received TG T_{reg} cell–depleted CD4$^+$ CD45RB^{lo} T cells compared with WT cells. Further complexity may derive from the fact that IL-17A/IFN-γ double–producing CD4 T cells Th17 + Th1 have been observed in colitis models and human inflammatory bowel disease (IBD) patients (Annunziato et al., 2007; Ahern et al., 2010). Further studies are required to understand which of these complex T cell subsets are modulated directly via IL-10.

Intestinal pathology induced by T_{reg} cell–depleted CD4$^+$ CD45RB^{lo} T cells requires IL-22

We previously reported a protective function of both IL-17A and IL-22 in the CD45RB^{hi} colitis model (Zenewicz et al., 2008; O'Connor et al., 2009). As shown in Fig. 6, transfer of T_{reg} cell–depleted CD45RB^{lo} CD4 T cells causes a more Th17 type of colitis compared with CD45RB^{hi} CD4$^+$ T cells. However, the role of IL-22 and IL-17A in this model was unclear. To analyze the role of these cytokines in the T_{reg} cell–depleted CD4$^+$ CD45RB^{lo} colitis, we performed adoptive transfer experiments using IL-17A– or IL-22–deficient T cells as donor cells. We again used CD25 as a marker to deplete T_{reg} cells within the CD45RB^{lo} CD4$^+$ T cells. CD25$^-$CD45RB^{lo} cells were purified as shown in Fig. S5 A. Transfer of IL-22 KO but not IL-17A KO T_{reg} cell–depleted CD4$^+$ CD45RB^{lo} T cells into Rag1 KO caused a reduced loss of body mass and histological colitis score compared with the mice that received WT cells (Fig. S5, B and C). We next aimed to study the role of T cell–derived IL-22 in more detail. First, we repeated that upon transfer into Rag1 KO mice, IL-22 KO T_{reg} cell–depleted CD4$^+$ CD45RB^{lo} T cells cause less disease based on mass loss, colon length, and endoscopic and histological colitis score compared with WT (Fig. 8, A–D).

Further analyses of the cytokine mRNA levels of the colon showed that colitis induced with IL-22 KO T_{reg} cell–depleted CD4$^+$ CD45RB^{lo} T cells was manifested by reduced

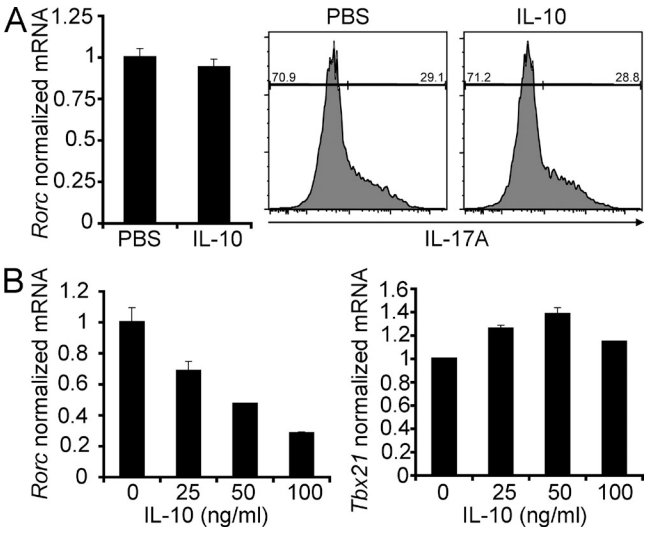

Figure 7. IL-10 does not inhibit the differentiation of naive T cells into Th17 cells but decreases *Rorc* expression in the T_{reg} cell–depleted CD45RB^{lo} T cells in vitro. (A) Naive T cells were cultured for 3 d in the presence of 0.5 ng/ml TGF-β1, 10 ng/ml IL-6, and 20 ng/ml IL-23. 100 ng recombinant IL-10 was added as indicated. *Rorc* mRNA levels normalized to HPRT are shown. IL-17A expression was measured using flow cytometry. (B) CD4$^+$Foxp3 RFP$^-$CD45RB^{lo} cells were sorted using FACS and were in vitro stimulated with IL-23 for 6 h in the presence of different concentrations of recombinant IL-10 as indicated. *Rorc* and *Tbx21* mRNA levels normalized to HPRT are shown. Results are representative of at least two independent experiments. Error bars represent mean ± SEM.

IFN-γ and IL-22 and similar TNF and IL-17A expression compared with WT controls (Fig. 8 E). Of note, in colitis, IL-22 can be produced by innate and adaptive immune cells (Zenewicz et al., 2008); therefore, IL-22 mRNA expression in the IL-22 KO T_{reg} cell–depleted CD4$^+$ CD45RB^{lo} T cell transfer model was still detectable but remarkably lower than in the mice that received the corresponding WT cells. This suggests that during colitis induced by T_{reg} cell–depleted CD4$^+$ CD45RB^{lo} T cells, most of the IL-22 expression derived from donor T cells or, less likely, that the T cells influence the production of IL-22 by the innate cells.

To further characterize the role of IL-22 in the development of colitis induced by T_{reg} cell–depleted CD4$^+$ CD45RB^{lo} T cells, we analyzed the expression of downstream molecules known to be induced by IL-22 such as Lipocalin 2 (Raffatellu et al., 2009), Mucin 1 (Sugimoto et al., 2008), and Reg3-γ (Zheng et al., 2008). Although Lipocalin 2 and Mucin 1 were not altered by the absence of IL-22 in donor T cells, Reg3-γ expression was greatly reduced in the colons in the mice that received IL-22 KO T_{reg} cell–depleted CD4$^+$ CD45RB^{lo} T cells compared with those that received WT corresponding cells (Fig. 8 F). As a C-type lectin antimicrobial molecule, Reg3-γ specifically binds and lyses Gram-positive but not Gram-negative bacteria (Cash et al., 2006). Selective alterations that disrupt the composition of the commensal flora may exacerbate colitis. These results suggest that the colitis induced with T_{reg} cell–depleted CD4$^+$ CD45RB^{lo} T cells might develop through an IL-22–Reg3-γ pathway. However, it is not clear whether the observed difference in Reg3-γ expression in the colon of IL-22 KO T_{reg} cell–depleted CD4$^+$ CD45RB^{lo} T cells is causally linked to the reduced intestinal disease or just a correlation with the reduced IL-22 levels. Further studies are required to address this point.

Interestingly, and in contrast to the CD45RB^{hi} transfer colitis model, the colitis induced by the transfer of T_{reg} cell–depleted CD4$^+$ CD45RB^{lo} T cells was not characterized by ulceration of the mucosa, but rather a pronounced thickening of the mucosa. Interestingly, IL-22 KO T_{reg} cell–depleted CD4$^+$ CD45RB^{lo} T cells did not cause this mucosal thickening and epithelial hyperplasia (Fig. 8 A and Fig. S7 D).

This difference suggested that IL-22 might be involved in the growth or survival of the colon epithelial cells as previously suggested by others (Pickert et al., 2009). We therefore analyzed the proliferation of epithelial cells. First, we assessed the BrdU incorporation in epithelial cells by immunohistochemistry: the number of BrdU-positive epithelial cells was significantly reduced in the colon of the Rag1 KO mice that had received IL-22 KO T_{reg} cell–depleted CD45RB^{lo} colitis compared with the controls (Fig. 9, A and B). These results were confirmed by the analyses of Ki67 expression and BrdU uptake using flow cytometry (Fig. S6). However, the differences observed did not seem to derive from an effect on cell survival because the number of apoptotic epithelial cells as detected by TdT-mediated dUTP-biotin nick end labeling (TUNEL) staining was not different in the presence or absence of IL-22 in the donor cells (Fig. 9 C). These results suggest that IL-22 from donor cells promotes proliferation of the colon epithelium, leading to mucosal hyperplasia and thickening.

Morphology of CD45RB^{hi} and T_{reg} cell–depleted CD45RB^{lo} CD4$^+$ T cell–driven colitis

When we compared colitis induced by WT CD45RB^{hi} cells and T_{reg} cell–depleted CD45RB^{lo} CD4$^+$ T cells, we noticed that the architecture of the gut epithelium was highly distorted in the CD45RB^{hi} transfer model (Fig. S7 B). In contrast, upon transfer of T_{reg} cell–depleted CD45RB^{lo}, the epithelia exhibited less damage but pronounced hyperplasia of the epithelium (Fig. 8 D and Fig. S7 B), leading to a significant thickening of the mucosal layer compared with the CD45RB^{hi} transfer model (Fig. S7 B). IFN-γ mRNA levels were increased in the colon in the CD45RB^{hi} colitis model, and this cytokine might be toxic to the colon epithelium. We therefore decided to analyze the involvement of this cytokine. We performed adoptive transfers of CD45RB^{hi} CD4$^+$ T cells from IFN-γ KO mice into Rag1 KO mice, and these mice lost mass and developed colitis upon transfer (Fig. S7, A and B). However, the destruction of the epithelial architecture was less severe, and the mucosa was more hyperplastic, causing increased thickening of the mucosal layer, which resembles the morphology of colitis induced with T_{reg} cell–depleted CD4$^+$ CD45RB^{lo} T cells (Fig. S7, B and D). The expression of IFN-γ was highly reduced in the colitis induced with IFN-γ KO

CD45RB^{hi} T cells compared with the corresponding WT cells (Fig. S7 C). In contrast, Th17 cytokines such as IL-22, IL-17A, and IL-17F were highly elevated, suggesting that Th17 but not Th1 cells are predominant in colitis developed with IFN-γ KO CD45RB^{hi} cells. In conclusion, these results suggested that the absence of IFN-γ or high expression of

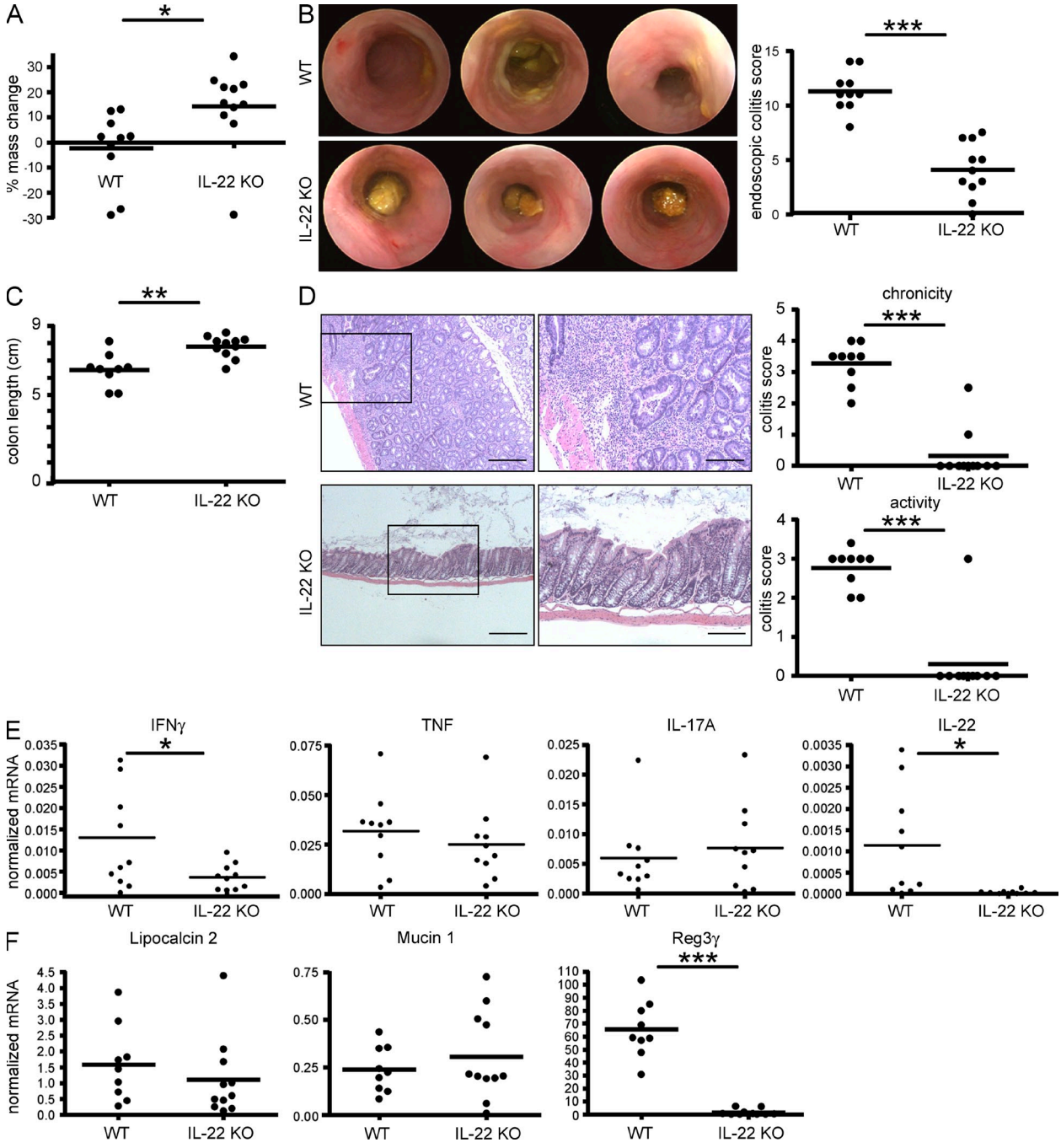

Figure 8. Intestinal pathology induced by CD25^{-}CD45RB^{lo} T cells is dependent on T cell–derived IL-22. CD4^{+}CD25^{-}CD45RB^{lo} (T_{reg} cell–depleted CD45RB^{lo}) cells from C57BL/6 (WT) or *Il22*$^{-/-}$ mice (IL-22 KO) were adoptively transferred into Rag1 KO mice. (A) Percent change from initial mouse weight 13 wk after cell transfer. (B) Selected images from endoscopic colonoscopies performed on the mice at 13 wk after transfer (left) and endoscopic colitis scores (right). (C) Graph represents colon length at 14 wk after transfer. (D) Colon tissue sections were examined by hematoxylin and eosin staining. Shown are representative colon tissues. Colon sections were scored according to the Materials and methods for chronicity (top) and disease activity (bottom). The boxed areas are shown at higher magnification on the right. Bars: (left) 1,000 µm; (right) 400 µm. (E) mRNA levels of different cytokines in the distal colon of the mice. (F) mRNA levels of the indicated IL-22–regulated genes. Each dot represents one mouse; horizontal bars indicate the mean. Results are representative of two experiments. *, P < 0.05; **, P < 0.01; ***, P < 0.001.

Th17 cytokines might result in less destruction of epithelial architecture but instead may lead to mucosal hyperplasia of the colon epithelium.

DISCUSSION

In this study, we have analyzed the role of IL-10 signaling in CD4 T cells by generating dominant-negative IL-10Rα TG mice. Our results indicated that direct IL-10 signals control colitis development, in particular when caused by the T_{reg} cell–depleted CD45RB^{lo} memory/effector CD4 T cell population. This has also spotlighted characteristic differences in the mechanism of colitis development mediated by CD45RB^{hi} cells or T_{reg} cell–depleted CD45RB^{lo} CD4$^+$ T cells.

It was previously reported by others that activation could reduce the expression of IL-10R1 (IL-10Rα) mRNA in human T cell clones (Liu et al., 1994). We found that although expression of mouse IL-10Rα is reduced upon activation, it recovered after 24–48 h both at the level of mRNA (not depicted) and cell surface protein expression (Fig. S1). In addition, the surface expression of IL-10Rα is detectable at any time of activation by flow cytometry. The IL-10Rα on the surface of T cells is functional after IL-10 stimulation as Stat3 phosphorylation occurs both in CD45RB^{hi} and CD45RB^{lo} CD4$^+$ T cells (Fig. S1). Together, these results suggested the existence of functional IL-10 signaling in mouse CD4 T cells.

The adoptive transfer model has been frequently used as a model of colitis, which resembles some features of Crohn's disease. It has been shown previously that nT_{reg} cells could protect against colitis induced by CD45RB^{hi} CD4 T cells, and it was also found that IL-10 is not required for this suppression (Asseman et al., 2003). Interestingly, however, normal mice that received anti–IL-10R antibody developed colitis (Asseman et al., 2003), which suggested that cells other than CD45RB^{hi} and nT_{reg} T cells may participate in the development of colitis. Our current results are in line with these findings and suggest that T_{reg} cell–depleted CD4$^+$ CD45RB^{lo} T cells are responsible for colitis under conditions where IL-10 is neutralized. In addition, TG T_{reg} cell–depleted CD4$^+$ CD45RB^{lo} T cells are not well controlled by nT_{reg} cells in vivo and in vitro in the presence of IL-23 (Figs. 3 and 4). Thus, blockade of IL-10 signaling might render T_{reg} cell–depleted CD45RB^{lo} CD4 T cells resistant to suppression by nT_{reg} cells and thus make recipient Rag1 KO mice susceptible to colitis.

The T_{reg} cell–depleted CD4$^+$ CD45RB^{lo} T cell population also contains IL-10–producing T cells, and it would therefore also be possible that blockade of IL-10 signaling led to a reduced number of IL-10–secreting cells. However, we could not find a significant difference in IL-10–producing cells upon transfer of T_{reg} cell–depleted CD4$^+$ CD45RB^{lo} T cells into Rag1 KO mice (WT, 1.4 ± 0.34% vs. TG, 2 ± 0.3%), indicating that IL-10 signaling is dispensable for the generation of IL-10–producing T cells, which is in line with a previous publication (Maynard et al., 2007). Since the preparation of this manuscript, an interesting manuscript was published that showed that IL-10 inhibits the function of nT_{reg} cells by repressing Foxp3 expression (Murai et al., 2009). Therefore, IL-10Rβ KO T_{reg} cells were not able to suppress CD4$^+$ CD45RB^{hi} T cells upon transfer into an immune-deficient host (Murai et al., 2009). The results in our model are primarily directed at an additional inhibitory function of IL-10 on the pathogenic effector/memory cells. In contrast to the study by Murai et al. (2009), we could not find any defect in the suppressive capacity of nT_{reg} cells with blocked IL-10 signaling in vivo or in vitro. Differences in the mouse model used may account for these different results. Additionally, current publications suggest a major role of the microbial milieu for the development of colitis (Round and Mazmanian, 2009; Nell et al., 2010), and therefore differences in the microbial milieu in the different animal facilities might also contribute to our different result.

Throughout our analysis, we also found that CD45RB^{hi} cells and T_{reg} cell–depleted CD45RB^{lo} CD4$^+$ T cells exhibit different characteristics when adoptively transferred into Rag1 KO mice (Fig. S8). CD45RB^{hi} cells proliferate more aggressively (Fig. S4 B) and induce colitis faster than T_{reg} cell–depleted CD45RB^{lo} cells. Additionally, the CD4 T cell effector response found in colitis developed by CD4$^+$ CD45RB^{hi} T cells was characterized by increased Th1 cytokines compared with T_{reg}

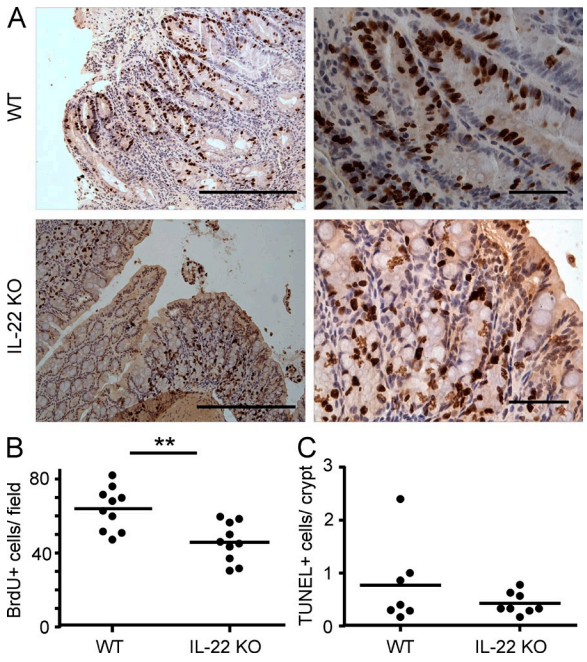

Figure 9. IL-22 promotes cell proliferation in the colon. CD4$^+$CD25$^-$CD45RB^{lo} (T_{reg} cell–depleted CD45RB^{lo}) cells from C57BL/6 (WT) or *Il22*$^{-/-}$ (IL-22 KO) mice were adoptively transferred into Rag1 KO mice. At 14 wk after transfer, 4 h before euthanization, mice were injected with BrdU. Colon sections were stained by immunohistochemistry with an antibody to BrdU. (A) Selected micrographs from two individual mice. Bars: (left) 250 µm; (right) 50 µm. (B) Quantification of the mean number of BrdU$^+$ cells per field for the sections in A. (C) Colonic tissue sections were also subjected to TUNEL staining. TUNEL$^+$ cells per crypt were quantified. Each dot represents one mouse; horizontal bars indicate the mean (BrdU: WT, n = 10; and KO, n = 10; TUNEL: WT, n = 7; and KO, n = 8). Results were confirmed twice using BrdU and Ki67 staining of colon epithelial cells and flow cytometry (shown in Fig. S6). **, P < 0.01.

cell–depleted $CD4^+$ $CD45RB^{lo}$ T cell–induced colitis, which was characterized more by Th17 cytokines. The blockade of IL-10 signaling selectively affected the T_{reg} cell–depleted $CD45RB^{lo}$ T cells, rendering them more pathological and enabling them to escape from control by nT_{reg} cells. We also analyzed whether IL-10 inhibits the in vitro differentiation of naive T cells into Th17. However, we could not find any significant inhibitory effect of IL-10 on the mRNA expression of *Rorc*, the gene encoding ROR-γt, or on the frequency of IL-17A–producing T cells generated from naive CD4T cells. In contrast, we found that IL-10 decreased, in a dose-dependent manner, the mRNA expression of *Rorc* but not *Tbx21*, the gene encoding T-bet, in IL-23–stimulated $CD45RB^{lo}$ T cells in vitro (Fig. 7). These data strengthen our in vivo data and suggest again that IL-10 is particularly important to control the antigen-experienced inflammatory cells.

Histologically, the $CD45RB^{hi}$ colitis model was characterized by ulceration, in contrast to the T_{reg} cell–depleted $CD45RB^{lo}$ colitis model, which instead showed epithelial hyperplasia and thickening of the mucosa. IL-22 was found to be protective in the $CD45RB^{hi}$ colitis model (Zenewicz et al., 2008) as well as in an ulcerative colitis model (Sugimoto et al., 2008) and to ameliorate inflammation during colon infection (Zheng et al., 2008). However, in contrast, in this study, we found a pathogenic role of this cytokine in the colitis model induced by T_{reg} cell–depleted $CD4^+$ $CD45RB^{lo}$ T cells.

High Th1 cytokines such as IFN-γ in the colon might be toxic to the colonic epithelium and might exacerbate disease, leading to the epithelial erosion and ulceration that characterizes the $CD45RB^{hi}$ model. Our finding that colitis induced with T cells from IFN-γ KO mice showed less epithelial damage supports this hypothesis. In line with this idea, we found that IL-17A KO $CD45RB^{hi}$ $CD4^+$ T cells cause more severe disease upon transfer into Rag1 KO recipients compared with WT. Interestingly, this was associated with increased IFN-γ–producing T cells and more severe ulceration in the mice receiving WT cells (O'Connor et al., 2009). In this context, it is possible that Th17 cytokines like IL-22 might protect the epithelium in the presence of Th1 cytokines. In contrast, in the T_{reg} cell–depleted $CD45RB^{lo}$ $CD4^+$ T cell adoptive transfer, IFN-γ expression in the colon was lower and Th17 cytokine mRNA levels, including IL-22 expression, were higher than in $CD45RB^{hi}$ model.

As the colonic epithelia were hyperplastic and the mucosal layer thickened in the T_{reg} cell–depleted $CD45RB^{lo}$ transfer model, the Th17 cytokine environment might be involved in the regeneration of epithelial cells. IL-22 might act on epithelial cells to promote proliferation or survival (Pickert et al., 2009). This seems to be beneficial in the $CD45RB^{hi}$ model through repair or prevention of epithelial erosion and ulceration. The observation that IL-22 KO T_{reg} cell–depleted $CD45RB^{lo}$ T cells showed milder intestinal pathology and less hyperplasia of the epithelia supports the hypothesis that, in contrast, IL-22, by precisely the same mechanism, might also lead to epithelial hyperproliferation and therefore could play a pathogenic role. Accordingly, in the literature, IL-22 has been reported to have dual proinflammatory and anti-inflammatory functions. IL-22 is required for skin inflammation and thickening in the IL-23–dependent model of psoriasis (Zheng et al., 2007; Ma et al., 2008), whereas it is protective in a hepatitis model (Zenewicz et al., 2007). The hyperproliferative pathology in psoriasis is comparable with the similar outcome in the T_{reg} cell–depleted $CD45RB^{lo}$ model. In conclusion, our results suggest that overproduction of IL-22, which is the case in the T_{reg} cell–depleted $CD45RB^{lo}$ colitis model, results in epithelial hyperplasia, which causes greater intestinal pathology and weight loss. However, we found that IFN-γ is also decreased in the absence of T cell–derived IL-22 in the T_{reg} cell–depleted $CD45RB^{lo}$ colitis model, and we therefore cannot exclude a possible contribution of IFN-γ to the pathogenesis in these settings. Further investigation on how this dual functionality of IL-22 is achieved should be elucidated and will lead to a better understanding of IBD. Our results also point to the complexity of using IL-22 antagonism or agonism in the therapy of inflammatory diseases.

In summary, our findings point to a fundamental difference in the pathological mechanisms that underlie colitis induced by $CD45RB^{hi}$ and T_{reg} cell–depleted $CD45RB^{lo}$ $CD4^+$ T cells, as the latter requires direct IL-10 signaling to be regulated by nT_{reg} cells. It is noteworthy that human Crohn's disease may well result from the action of memory/effector (T_{reg} cell–depleted $CD45RB^{lo}$) T cells rather than or as well as $CD45RB^{hi}$ $CD4^+$ T cells. In any event, we believe that this new model for IBD provides a useful additional alternative to the already existing portfolio of IBD models, and further investigation of this model might contribute to the search for a cure or better treatment of human IBD.

MATERIALS AND METHODS

Mice and reagents. C57BL/6 mice and CD45.1 mice were purchased from the National Cancer Institute. IL-10, IFN-γ, and Rag1 KO mice were obtained from the Jackson Laboratory. Foxp3 knockin reporter (FIR) mice (Wan and Flavell, 2005), IL-17A KO (Nakae et al., 2002), and IL-22 KO (Zenewicz et al., 2007) mice have been described previously. Our Rag1 KO colony tested PCR positive for *Helicobacter hepaticus* (Shames et al., 1995). All animal procedures were approved by the Institutional Animal Care and Use Committee of Yale University. Recombinant IL-10 and antibodies to IL-10Rα, B220, CD4, CD8 CD11b, and CD11c were purchased from BD.

Generation of CD4dnIL-10Rα mice. The mouse IL-10Rα gene fragment truncated at proline 265 just beneath the transmembrane region was cloned by PCR from cDNA generated from mouse B cell mRNA. The primer of this reaction was flanked with SalI sites, and the fragment was subcloned into the SalI site of plasmid CD4 promoter vector p37.1 (Gorelik and Flavell, 2000). The truncated form of IL-10Rα has ∼10 residues of read through amino acids at the carboxy terminal, which derive from the vector sequence before a termination codon. To generate TG mice, the CD4dnIL-10Rα fragment containing CD4 promoter, IL-10Rα, and polyadenylation sequence was excised by NotI, purified, and injected into $(C57BL/6xC3H)F_1$-fertilized eggs. Founder mice were identified using PCR and backcrossed at least 12 times onto the C57BL/6 background for further experiments.

Western blot. For the analysis of Stat3 phosphorylation, total cell lysates of the indicated cell populations were separated on a 10% SDS gel, transferred to a polyvinylidene fluoride membrane (Millipore) and probed with anti–phospho-Stat3 (Tyr705) antibody (Cell Signaling Technology). The membrane

was stripped with 0.1 M glycine, pH 2.5, for 30 min at room temperature and reprobed with antibodies to total Stat3 (Cell Signaling Technology).

Flow cytometry. 10^6 cells from spleen, lymph nodes, or thymus were first preincubated with 2.4G2 mAb to block FcγR and then incubated with the indicated antibodies for 30 min on ice. The samples were washed and analyzed on FACSCaliber (BD), and 20,000 live cell events were collected. The analyses were conducted using FlowJo (Tree Star) analysis software. All antibodies used for staining were obtained from BD.

For intracellular cytokine staining, single-cell suspensions of spleen or lymph node cells were stimulated with 50 ng/ml PMA (Sigma-Aldrich) and 1 mM ionomycin (Sigma-Aldrich) for 4 h; monensin (BD) was added for the last 2 h of stimulation of the culture. After stimulation, cells were stained with a mixture of Cy-chrome–labeled anti-CD4 and biotinylated anti-CD8 mAbs, subsequently fixed and permeabilized using a Cytofix/Cytoperm kit (BD), and then stained using FITC-labeled anti–IFN-γ mAb and PE-labeled anti–IL-17A mAb and streptavidin-APC (all from BD) according to the manufacturer's recommendations. Isotype-matched FITC- or PE-labeled mAbs were used as negative control for intracellular cytokine staining. 50,000 events were collected, and after gating on $CD4^+$ or $CD8^+$ cells, intracellular cytokine staining was analyzed. Gates for cytokine staining were set using isotype-matched control antibody staining. The intracellular staining of Ror-γt and Foxp3 was performed similarly according to the manufacturer's instruction (eBioscience).

Proliferation assay. In vitro proliferation assay was performed essentially as described previously (Takahashi et al., 2000). In brief, 2×10^4 responder cells ($CD45RB^{hi}$ or $CD45RB^{lo}$ cells) and 5×10^4 irradiated splenocytes (APC) were cultured with varying number of $Foxp3^+$ nT_{reg} cells and anti-CD3 (145-2C11) in a 96-well plate for 3 d. We added 20 ng/ml IL-23 (eBioscience) to some of the wells. Incorporation of $[^3H]$TdR (1 μCi/well) by proliferating lymphocytes during the last 6 h of the culture was measured.

Adoptive transfer and IBD model. Splenocytes were collected from 8–12-wk-old CD4dnIL-10Rα mice or control WT mice or IL-17A KO, IFN-γ KO, or IL-22 KO mice, and the CD4-positive cells were isolated by MACS system (Miltenyi Biotec) by positive selection according to the manufacturer's instruction. The purity of $CD4^+$ T cells obtained was >90% determined by FACS. In some experiments, we further sorted the $CD4^+$ T cells to collect $CD45RB^{hi}$, $Foxp3^-(CD25^-)CD45RB^{lo}$ (T_{reg} cell–depleted $CD45RB^{lo}$), and $Foxp3^+(CD25^+)$ nT_{reg} cells using FACS Vantage.

10^6 cells of CD4 T cells or 3×10^5 $CD25^-CD45RB^{lo}$ or $CD45RB^{hi}$ cells with or without 10^5 nT_{reg} cells were intravenously injected into Rag1 KO mice (The Jackson Laboratory). The mice were weighed once a week to monitor IBD development.

For competitive adoptive transfer experiment, we injected equal numbers (3×10^5) of WT (CD45.2 homozygote) and CD4dnIL-10Rα ($CD45.2^+$/$CD45.1^+$) $CD45RB^{hi}$ or $CD45RB^{lo}$ cells into CD45.1 Rag1 KO mice. 1 mo later, BrdU was fed and detected in the spleen, and mesenteric lymphocytes and intracellular IL-17A were detected.

Endoscopic procedure. Colonoscopy was performed in a blinded fashion for colitis scoring using the Coloview system (Karl Storz) as previously described (Becker et al., 2007). In brief, colitis scoring was based on granularity of the mucosal surface, stool consistency, vascular pattern, translucency of the colon, and visible fibrin (0–3 points for each).

Histological analysis. Tissue was fixed with 10% neutral formalin, paraffin embedded, sectioned at 3–6 μm, and stained with hematoxylin and eosin. For the colitis model, sections were blindly analyzed by a trained gastroenteropathologist. Each segment was given a score of 0–4: grade 0, no significant changes; grade 1, minimal scattered mucosal inflammatory cell infiltrates, with or without minimal epithelial hyperplasia; grade 2, mild scattered to diffuse inflammatory cell infiltrates, sometimes extending into the submucosa and associated with erosions, with mild to moderate epithelial hyperplasia and mild to moderate mucin depletion from goblet cells; grade 3, moderate inflammatory cell infiltrates that were sometimes transmural, with moderate to severe epithelial hyperplasia and mucin depletion; grade 4, marked inflammatory cell infiltrates that were often transmural and associated with crypt abscesses and occasional ulceration, with marked epithelial hyperplasia, mucin depletion, and loss of intestinal glands. For the IL-22 experiments, chronicity (the degree of chronic inflammation) and activity (degree of epithelial injury) were scored separately.

Quantitative PCR. RNA was extracted with TRIZOL reagent, and cDNA was synthesized by Superscript II reverse-transcriptase according to the manufacturer's protocols (Invitrogen). The real-time PCR system (model 7500; Applied Biosystems) was used for quantitative PCR. The sequence of the probe to detect IFN-γ was 5′-FAM-TTTGAGGTCAACAACCCACAGGTCCA-BHQ-1-3′with the primers, 5′-CCTTTTCCGCTTCCTGAGG-3′ and 5′-CTGGTGAAAAGGACCTCTCG-3′. The primer probe sets for IL-10Rα (Mm00434151_m1), IL-17A (Mm00434291_m1), IL-17F (Mm00521423_m1), IL-22 (Mm00444241_m1), and G-CSF (Mm00438334_m1) were purchased from Applied Biosystems. Hypoxanthine phosphoribosyltransferase (HPRT) was used as an internal reference and measured with the primers 5′-CTGGTGAAAAGGACCTCTCG-3′ and 5′-TGAAGTACTCATTATAGTCAAGGGCA-3′ with the TaqMan probe 5′-FAM-TGTTGGATACAGGCCAGACTTTGTTGGAT-BHQ-1-3′. Relative expression of cytokines normalized to HPRT was calculated using the ΔΔCt method. The relative fold changes of expression are presented, where control samples are set to an expression index of 1.

Statistical analysis. Survival rate was analyzed by logrank test, and histology score was determined by the Mann-Whitney *U* test. Other data were analyzed by the Student's *t* test.

Online supplemental material. Fig. S1 shows expression of IL-10Rα in murine CD4 T cells. Fig. S2 shows that IL-6–mediated Stat3 activation is not abrogated in TG CD4 T cells. Fig. S3 characterizes the TG $Foxp3^-CD45RB^{lo}$ cells before adoptive transfer. Fig. S4 shows the competitive adoptive transfer of WT and TG $CD45RB^{hi}$ or $CD25^-CD45RB^{lo}$ cells into Rag1 KO mice. Fig. S5 shows that induction of colitis by $CD25^-CD45RB^{lo}$ cells is dependent on T cell–derived IL-22 but not IL-17A. Fig. S6 shows increased epithelial cell proliferation in Rag1 KO mice receiving IL-22 KO $CD25^-CD45RB^{lo}$ cells using flow cytometry. Fig. S7 characterizes colitis induced by the transfer of IFN-γ KO $CD45RB^{hi}$ T cells into Rag1 KO mice. Fig. S8 is a summary of the colitis developed by $CD45RB^{hi}$ and T_{reg} cell–depleted $CD45RB^{lo}$ T cells. Online supplemental material is available at http://www.jem.org/cgi/content/full/jem.20102149/DC1.

We thank Fran Manzo for assistance with manuscript preparation, Cindy Hughes and Debbie Butkus for the generation of TG mice, and Elizabeth Eynon for managing the mouse program.

This work was supported by National Institutes of Health awards AI36529 and DK45735 (to R.A. Flavell). S. Huber was supported by the Deutsche Forschungsgemeinschaft (HU 1714/1-1) and by a James Hudson Brown–Alexander B. Coxe Fellowship. L.A. Zenewicz was supported by a postdoctoral fellowship from the American Cancer Society. R.A. Flavell is an Investigator of the Howard Hughes Medical Institute.

The authors have no competing financial interests.

Submitted: 30 September 2010
Accepted: 21 March 2011

REFERENCES

Ahern, P.P., C. Schiering, S. Buonocore, M.J. McGeachy, D.J. Cua, K.J. Maloy, and F. Powrie. 2010. Interleukin-23 drives intestinal inflammation through direct activity on T cells. *Immunity*. 33:279–288. doi:10.1016/j.immuni.2010.08.010

Annunziato, F., L. Cosmi, V. Santarlasci, L. Maggi, F. Liotta, B. Mazzinghi, E. Parente, L. Filì, S. Ferri, F. Frosali, et al. 2007. Phenotypic and functional features of human Th17 cells. *J. Exp. Med.* 204:1849–1861. doi:10.1084/jem.20070663

Asseman, C., S. Mauze, M.W. Leach, R.L. Coffman, and F. Powrie. 1999. An essential role for interleukin 10 in the function of regulatory T cells

that inhibit intestinal inflammation. *J. Exp. Med.* 190:995–1004. doi:10.1084/jem.190.7.995

Asseman, C., S. Read, and F. Powrie. 2003. Colitogenic Th1 cells are present in the antigen-experienced T cell pool in normal mice: control by CD4+ regulatory T cells and IL-10. *J. Immunol.* 171:971–978.

Becker, C., M.C. Fantini, and M.F. Neurath. 2007. High resolution colonoscopy in live mice. *Nat. Protoc.* 1:2900–2904. doi:10.1038/nprot.2006.446

Cash, H.L., C.V. Whitham, C.L. Behrendt, and L.V. Hooper. 2006. Symbiotic bacteria direct expression of an intestinal bactericidal lectin. *Science*. 313:1126–1130. doi:10.1126/science.1127119

Ding, L., and E.M. Shevach. 1992. IL-10 inhibits mitogen-induced T cell proliferation by selectively inhibiting macrophage costimulatory function. *J. Immunol.* 148:3133–3139.

Ding, L., P.S. Linsley, L.Y. Huang, R.N. Germain, and E.M. Shevach. 1993. IL-10 inhibits macrophage costimulatory activity by selectively inhibiting the up-regulation of B7 expression. *J. Immunol.* 151:1224–1234.

Duerr, R.H., K.D. Taylor, S.R. Brant, J.D. Rioux, M.S. Silverberg, M.J. Daly, A.H. Steinhart, C. Abraham, M. Regueiro, A. Griffiths, et al. 2006. A genome-wide association study identifies IL23R as an inflammatory bowel disease gene. *Science*. 314:1461–1463. doi:10.1126/science.1135245

Fiorentino, D.F., A. Zlotnik, P. Vieira, T.R. Mosmann, M. Howard, K.W. Moore, and A. O'Garra. 1991. IL-10 acts on the antigen-presenting cell to inhibit cytokine production by Th1 cells. *J. Immunol.* 146:3444–3451.

Gazzinelli, R.T., I.P. Oswald, S.L. James, and A. Sher. 1992. IL-10 inhibits parasite killing and nitrogen oxide production by IFN-gamma-activated macrophages. *J. Immunol.* 148:1792–1796.

Gorelik, L., and R.A. Flavell. 2000. Abrogation of TGFbeta signaling in T cells leads to spontaneous T cell differentiation and autoimmune disease. *Immunity*. 12:171–181. doi:10.1016/S1074-7613(00)80170-3

Kamanaka, M., S.T. Kim, Y.Y. Wan, F.S. Sutterwala, M. Lara-Tejero, J.E. Galán, E. Harhaj, and R.A. Flavell. 2006. Expression of interleukin-10 in intestinal lymphocytes detected by an interleukin-10 reporter knockin tiger mouse. *Immunity*. 25:941–952. doi:10.1016/j.immuni.2006.09.013

Kühn, R., J. Löhler, D. Rennick, K. Rajewsky, and W. Müller. 1993. Interleukin-10-deficient mice develop chronic enterocolitis. *Cell*. 75:263–274. doi:10.1016/0092-8674(93)80068-P

Liu, Y., S.H. Wei, A.S. Ho, R. de Waal Malefyt, and K.W. Moore. 1994. Expression cloning and characterization of a human IL-10 receptor. *J. Immunol.* 152:1821–1829.

Ma, H.L., S. Liang, J. Li, L. Napierata, T. Brown, S. Benoit, M. Senices, D. Gill, K. Dunussi-Joannopoulos, M. Collins, et al. 2008. IL-22 is required for Th17 cell-mediated pathology in a mouse model of psoriasis-like skin inflammation. *J. Clin. Invest.* 118:597–607.

MacNeil, I.A., T. Suda, K.W. Moore, T.R. Mosmann, and A. Zlotnik. 1990. IL-10, a novel growth cofactor for mature and immature T cells. *J. Immunol.* 145:4167–4173.

Maynard, C.L., L.E. Harrington, K.M. Janowski, J.R. Oliver, C.L. Zindl, A.Y. Rudensky, and C.T. Weaver. 2007. Regulatory T cells expressing interleukin 10 develop from Foxp3+ and Foxp3- precursor cells in the absence of interleukin 10. *Nat. Immunol.* 8:931–941. doi:10.1038/ni1504

Murai, M., O. Turovskaya, G. Kim, R. Madan, C.L. Karp, H. Cheroutre, and M. Kronenberg. 2009. Interleukin 10 acts on regulatory T cells to maintain expression of the transcription factor Foxp3 and suppressive function in mice with colitis. *Nat. Immunol.* 10:1178–1184. doi:10.1038/ni.1791

Nakae, S., Y. Komiyama, A. Nambu, K. Sudo, M. Iwase, I. Homma, K. Sekikawa, M. Asano, and Y. Iwakura. 2002. Antigen-specific T cell sensitization is impaired in IL-17-deficient mice, causing suppression of allergic cellular and humoral responses. *Immunity*. 17:375–387. doi:10.1016/S1074-7613(02)00391-6

Nell, S., S. Suerbaum, and C. Josenhans. 2010. The impact of the microbiota on the pathogenesis of IBD: lessons from mouse infection models. *Nat. Rev. Microbiol.* 8:564–577. doi:10.1038/nrmicro2403

O'Connor, W. Jr., M. Kamanaka, C.J. Booth, T. Town, S. Nakae, Y. Iwakura, J.K. Kolls, and R.A. Flavell. 2009. A protective function for interleukin 17A in T cell-mediated intestinal inflammation. *Nat. Immunol.* 10:603–609. doi:10.1038/ni.1736

Pickert, G., C. Neufert, M. Leppkes, Y. Zheng, N. Wittkopf, M. Warntjen, H.A. Lehr, S. Hirth, B. Weigmann, S. Wirtz, et al. 2009. STAT3 links IL-22 signaling in intestinal epithelial cells to mucosal wound healing. *J. Exp. Med.* 206:1465–1472. doi:10.1084/jem.20082683

Powrie, F., R. Correa-Oliveira, S. Mauze, and R.L. Coffman. 1994. Regulatory interactions between CD45RBhigh and CD45RBlow CD4+ T cells are important for the balance between protective and pathogenic cell-mediated immunity. *J. Exp. Med.* 179:589–600. doi:10.1084/jem.179.2.589

Raffatellu, M., M.D. George, Y. Akiyama, M.J. Hornsby, S.P. Nuccio, T.A. Paixao, B.P. Butler, H. Chu, R.L. Santos, T. Berger, et al. 2009. Lipocalin-2 resistance confers an advantage to *Salmonella enterica* serotype *Typhimurium* for growth and survival in the inflamed intestine. *Cell Host Microbe*. 5:476–486. doi:10.1016/j.chom.2009.03.011

Round, J.L., and S.K. Mazmanian. 2009. The gut microbiota shapes intestinal immune responses during health and disease. *Nat. Rev. Immunol.* 9:313–323. doi:10.1038/nri2515

Sawada, S., J.D. Scarborough, N. Killeen, and D.R. Littman. 1994. A lineage-specific transcriptional silencer regulates CD4 gene expression during T lymphocyte development. *Cell*. 77:917–929. doi:10.1016/0092-8674(94)90140-6

Schandené, L., C. Alonso-Vega, F. Willems, C. Gérard, A. Delvaux, T. Velu, R. Devos, M. de Boer, and M. Goldman. 1994. B7/CD28-dependent IL-5 production by human resting T cells is inhibited by IL-10. *J. Immunol.* 152:4368–4374.

Shames, B., J.G. Fox, F. Dewhirst, L. Yan, Z. Shen, and N.S. Taylor. 1995. Identification of widespread *Helicobacter hepaticus* infection in feces in commercial mouse colonies by culture and PCR assay. *J. Clin. Microbiol.* 33:2968–2972.

Sugimoto, K., A. Ogawa, E. Mizoguchi, Y. Shimomura, A. Andoh, A.K. Bhan, R.S. Blumberg, R.J. Xavier, and A. Mizoguchi. 2008. IL-22 ameliorates intestinal inflammation in a mouse model of ulcerative colitis. *J. Clin. Invest.* 118:534–544.

Taga, K., B. Cherney, and G. Tosato. 1993. IL-10 inhibits apoptotic cell death in human T cells starved of IL-2. *Int. Immunol.* 5:1599–1608. doi:10.1093/intimm/5.12.1599

Takahashi, T., T. Tagami, S. Yamazaki, T. Uede, J. Shimizu, N. Sakaguchi, T.W. Mak, and S. Sakaguchi. 2000. Immunologic self-tolerance maintained by $CD25^+CD4^+$ regulatory T cells constitutively expressing cytotoxic T lymphocyte–associated antigen 4. *J. Exp. Med.* 192:303–310. doi:10.1084/jem.192.2.303

Veldhoen, M., R.J. Hocking, C.J. Atkins, R.M. Locksley, and B. Stockinger. 2006. TGFbeta in the context of an inflammatory cytokine milieu supports de novo differentiation of IL-17-producing T cells. *Immunity*. 24:179–189. doi:10.1016/j.immuni.2006.01.001

Wan, Y.Y., and R.A. Flavell. 2005. Identifying Foxp3-expressing suppressor T cells with a bicistronic reporter. *Proc. Natl. Acad. Sci. USA*. 102:5126–5131. doi:10.1073/pnas.0501701102

Ye, P., F.H. Rodriguez, S. Kanaly, K.L. Stocking, J. Schurr, P. Schwarzenberger, P. Oliver, W. Huang, P. Zhang, J. Zhang, et al. 2001. Requirement of interleukin 17 receptor signaling for lung CXC chemokine and granulocyte colony-stimulating factor expression, neutrophil recruitment, and host defense. *J. Exp. Med.* 194:519–527. doi:10.1084/jem.194.4.519

Zenewicz, L.A., G.D. Yancopoulos, D.M. Valenzuela, A.J. Murphy, M. Karow, and R.A. Flavell. 2007. Interleukin-22 but not interleukin-17 provides protection to hepatocytes during acute liver inflammation. *Immunity*. 27:647–659. doi:10.1016/j.immuni.2007.07.023

Zenewicz, L.A., G.D. Yancopoulos, D.M. Valenzuela, A.J. Murphy, S. Stevens, and R.A. Flavell. 2008. Innate and adaptive interleukin-22 protects mice from inflammatory bowel disease. *Immunity*. 29:947–957. doi:10.1016/j.immuni.2008.11.003

Zheng, Y., D.M. Danilenko, P. Valdez, I. Kasman, J. Eastham-Anderson, J. Wu, and W. Ouyang. 2007. Interleukin-22, a T(H)17 cytokine, mediates IL-23-induced dermal inflammation and acanthosis. *Nature*. 445:648–651. doi:10.1038/nature05505

Zheng, Y., P.A. Valdez, D.M. Danilenko, Y. Hu, S.M. Sa, Q. Gong, A.R. Abbas, Z. Modrusan, N. Ghilardi, F.J. de Sauvage, and W. Ouyang. 2008. Interleukin-22 mediates early host defense against attaching and effacing bacterial pathogens. *Nat. Med.* 14:282–289. doi:10.1038/nm1720

Zhong, Z., Z. Wen, and J.E. Darnell Jr. 1994. Stat3: a STAT family member activated by tyrosine phosphorylation in response to epidermal growth factor and interleukin-6. *Science*. 264:95–98. doi:10.1126/science.8140422